Science of the Total Environment 949 (2024) 174951

Contents lists available at ScienceDirect

Science of the Total Environment

journal homepage: www.elsevier.com/locate/scitotenv

Assessing controls on sedimentation rates and sediment organic carbon accretion in beaver ponds

J.C. Rees [a,*], K.B. Lininger [a], J.D. Landis [b], C.E. Briles [c]

[a] Department of Geography, University of Colorado Boulder, Boulder, CO 80309-0260, USA
[b] Department of Earth Sciences, Dartmouth College, Hanover, NH 03755, USA
[c] Department of Geography and Environmental Sciences, University of Colorado Denver, Denver, CO 80217-3364, USA

HIGHLIGHTS

- Determined sedimentation rates, depths, and sediment OC content in 45 beaver ponds
- Sedimentation rate was strongly negatively correlated with pond age.
- Sediment OC content was correlated with sediment grain size.
- Pond sediment in incised reaches likely has scoured and filled over time.
- Simulations suggest reconnecting incised channels to floodplains takes >100 yrs.

GRAPHICAL ABSTRACT

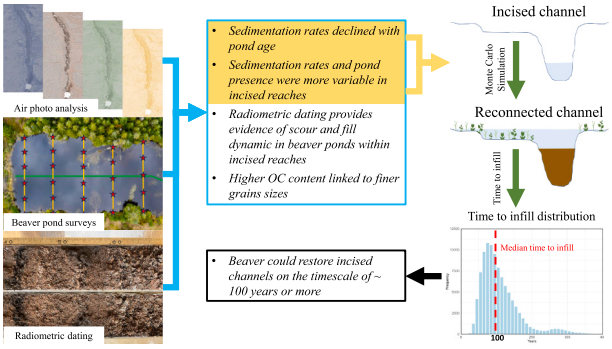

ARTICLE INFO

Editor: Paulo Pereira

Keywords:
Beaver
Critical zone
River corridors
Fluvial geomorphology
Sediment storage
Rivers and the carbon cycle

ABSTRACT

Beaver dams trap sediment, promote channel-floodplain connectivity, modify biogeochemical cycling and organic carbon (OC) storage, and influence geomorphic form. Beaver-related sediment accumulation has been investigated at longer timescales (e.g., > 1000 years) and shorter timescales (< 10 years), but we lack information on sedimentation and sediment-associated OC accretion rates over multiple decades in relatively persistent beaver ponds (10–100 years old). We coupled field surveys of 45 beaver ponds with historical aerial imagery and radiometric dating with ^{7}Be, ^{210}Pb, and ^{14}C to calculate sedimentation rates, mean sediment depth, and sediment OC content at two study sites in the southern Rocky Mountains, USA. Sedimentation rates in beaver ponds (median = 5.7 cm yr^{-1}, mean = 11.6 cm yr^{-1}) decreased with pond age. Incised, single threaded reaches had greater variability in mean sediment depth compared to less incised reaches. In less incised reaches, mean sediment depth and beaver dam height increased with pond age, indicating more stable dams and depositional environments. Sediment OC content within beaver ponds (median = 0.8 %, mean = 1.7 %) increased with finer sediment grain size distributions. Sediment OC accretion rates in ponds ranged between 0.13 and 23 Mg C ha $^{-1}$ per year. We used Monte Carlo simulations to estimate it would take ~100 years or more of uninhibited beaver activity for deposition to laterally reconnect adjacent terraces in the incised study reaches, a common objective within many stream restoration projects. Our findings show that beaver ponds in complex, multi-threaded reaches better retain fine sediment over longer timescales, highlighting the need to incorporate geomorphic

* Corresponding author at: Department of Geography, University of California, Santa Barbara, Ellison Hall, Santa Barbara, CA 93106, USA.
E-mail address: jamesrees@ucsb.edu (J.C. Rees).

https://doi.org/10.1016/j.scitotenv.2024.174951
Received 24 April 2024; Received in revised form 2 July 2024; Accepted 20 July 2024
Available online 26 July 2024

context when considering whether beaver can help restore incised river channels and floodplain connectivity, retain fine sediment, and store OC on the landscape.

1. Introduction

Between the 16th and 19th centuries, humans intensely altered river corridors in North America through the drastic reduction of the North American beaver (*Castor canadensis*) population (Butler and Malanson, 1995). Known as nature's "ecosystem engineers," beaver can initiate channel widening and sediment aggradation, enhance channel-floodplain connectivity, promote higher water tables, increase geomorphic heterogeneity, and create or improve wetland habitat and organic carbon (OC) storage (Brazier et al., 2021; Cluer and Thorne, 2014; Larsen et al., 2021; Pollock et al., 2014). Most studies on the impact of beaver on sedimentation in river corridors (including the channel, floodplain, and hyporheic zone (Harvey and Gooseff, 2015)) have measured young ponds (~5 years old or less), which are characterized by very high vertical sedimentation rates (R_{sed}) of 10–100 cm yr^{-1} (Butler and Malanson, 1995; Giriat et al., 2016; John and Klein, 2004; Pollock et al., 2014; Puttock et al., 2018). In contrast, studies of longer-term R_{sed} over Holocene timescales (10^3–10^4 years) estimate much lower mean R_{sed} of 0.01–0.1 cm yr^{-1} for beaver-meadow complexes, which include the channels, floodplains, and valley-bottoms that occur in broad, low-gradient valleys affected by beaver activity (Ives, 1942; Kramer et al., 2012; Persico and Meyer, 2009; Polvi and Wohl, 2012; Westbrook et al., 2011). However, R_{sed}, the factors that influence those rates, and OC accretion due to sedimentation in beaver ponds have not been sufficiently examined over intermediate timescales (~10–100 years old, hereafter referred to as "multidecade") that are particularly relevant to watershed management and planning. Only a few studies of stored sediment depths in beaver ponds have included multidecade ponds, and these studies either do not report R_{sed} (sediment depths are typically reported without rates) or have limited sample sizes (Butler, 2012; Butler and Malanson, 1995; Devito and Dillon, 1993; Meentemeyer and Butler, 1999; Pollock et al., 2007).

Multiple factors have been shown to influence R_{sed} and mean sediment depth (D_{sed}) within beaver-mediated river corridors. Watershed-scale controls may include drainage area, relief, and lithology (Larsen et al., 2021). At the reach scale, ponds located in reaches with higher stream power during floods experience more frequent dam breaching and less sediment retention over time (Levine and Meyer, 2014). Beaver ponds within steeper reaches tend to have less storage capacity than less steep reaches, given the same dam height (Pollock et al., 2003). Some studies have looked at sediment storage and transport within cascades or series of beaver ponds and found few downstream trends, likely because repeated dam breaches rework or homogenize sediment deposits within the cascade (Bigler et al., 2001; Levine and Meyer, 2014; Puttock et al., 2018; de Visscher et al., 2014). However, there have been fewer comparisons of beaver pond sedimentation rates between river corridor reaches with differing geomorphic form (e.g., incised reaches compared to beaver meadows), limiting our understanding of reach-specific geomorphic conditions that promote sediment persistence and retention over time.

At the local- (i.e., pond) scale, R_{sed} typically decreases with pond age (Butler and Malanson, 1995; Pollock et al., 2007). This observed relationship may result from pond widening over time, distributing sediment deposition over a larger area (Butler and Malanson, 1995), or pond abandonment; inhabited beaver ponds aggregate sediment and OC more rapidly than abandoned ponds because beaver actively input sediment, store organic material, and maintain dams (Hood and Larson, 2015; McCreesh et al., 2019; Puttock et al., 2018). In addition to pond age, pond geometry may influence sedimentation. For example, ponds with larger volumes and surface areas generally have higher D_{sed} (de Visscher et al., 2014; Giriat et al., 2016). Despite previous studies assessing factors that influence sedimentation, field-derived relationships between sedimentation rates and controlling variables often lack sufficient sample size or data from more persistent, multidecade ponds.

In addition to influencing sediment storage in river corridors, the presence of beaver can increase sediment OC content (% OC by mass) and stock (Mg OC ha^{-1}) when compared to reaches unimpacted by beaver (Cazzolla Gatti et al., 2018; Johnston, 2014; Murray et al., 2021; Naiman et al., 1986; Wohl, 2013). Even in cases where sediment OC content does not differ between beaver impacted and non-beaver impacted reaches, the greater depth of sediment within beaver-impacted reaches resulted in greater overall OC stock (Sutfin et al., 2021). Other studies have reported a positive association between pond age and sediment OC content (Butler and Malanson, 1995; Murray et al., 2021) due to continuous biotic inputs from beaver activity and improved preservation and storage of organic matter inundated by the beaver pond (Butler and Malanson, 1995; Laurel and Wohl, 2019). However, we lack understanding of sediment-associated OC accretion rates across ponds of differing ages, which limits our ability to account for altering carbon fluxes related to beaver removal or reintroduction (Cazzolla Gatti et al., 2018; Nummi et al., 2018; Wohl, 2013).

Here, we assess linkages between beaver pond age and characteristics, sedimentation, and OC content and accretion rates in two montane river corridors in the southern Rocky Mountains, USA. Our first research objective *(O1)* was to identify factors influencing R_{sed}, D_{sed}, and OC content in beaver ponds using field and geospatial data, radiometric dating, and statistical analyses. Our second research objective *(O2)* was to use equations for R_{sed} (developed through *O1* above) along with empirical distributions of pond age and the fraction of time beaver ponds are inundated to estimate the timescales at which beaver-related sedimentation could reconnect incised channels with abandoned floodplains (terraces). Our findings inform our understanding of how beaver influence sediment and OC storage in river corridors, with implications for river restoration practitioners and management agencies interested in implementing beaver-based restoration strategies.

2. Methods

2.1. Study sites

We conducted field work during spring and summer 2022 at Trout Creek (TC) west of Colorado Springs, Colorado, USA (Fig. 1a), and Coal Creek (CC) near Crested Butte, Colorado, USA (Fig. 1b). Both sites host active beaver populations and have long histories of beaver activity.

Trout Creek is within the upper South Platte River Basin and flows through portions of the Manitou Experimental Forest, draining a north-south trending valley formed by the Ute Pass Fault. The beaver ponds are underlain by Quaternary alluvium over bedrock composed of the Fountain Formation (arkosic sandstone), but most of the bedrock in the watershed is the granitic Pikes Peak Batholith (Tweto, 1979). The study area has an average annual precipitation of 430 mm, with approximately 50 % falling as rain (Frank et al., 2021; Ortega et al., 2014) mostly in the summer, often in the form of intense thunderstorms (Adams et al., 2008; Bush et al., 2023). Winter snowfall is typically low (Adams et al., 2008; Ortega et al., 2014), but peak flows occur in late spring and early summer from snowmelt (USGS Gage Data, 2022). Trout Creek discharge from a USGS gage located just downstream of the Trout Creek study area is available from October 2003 to October 2021 (USGS Gage Data, 2022), but was not used in this study because it is separated from the surveyed Trout Creek study area by an impoundment. We conducted surveys of three reaches along Trout Creek. TC01 is located upstream of Manitou Park Lake, a 2-ha earthen embankment reservoir

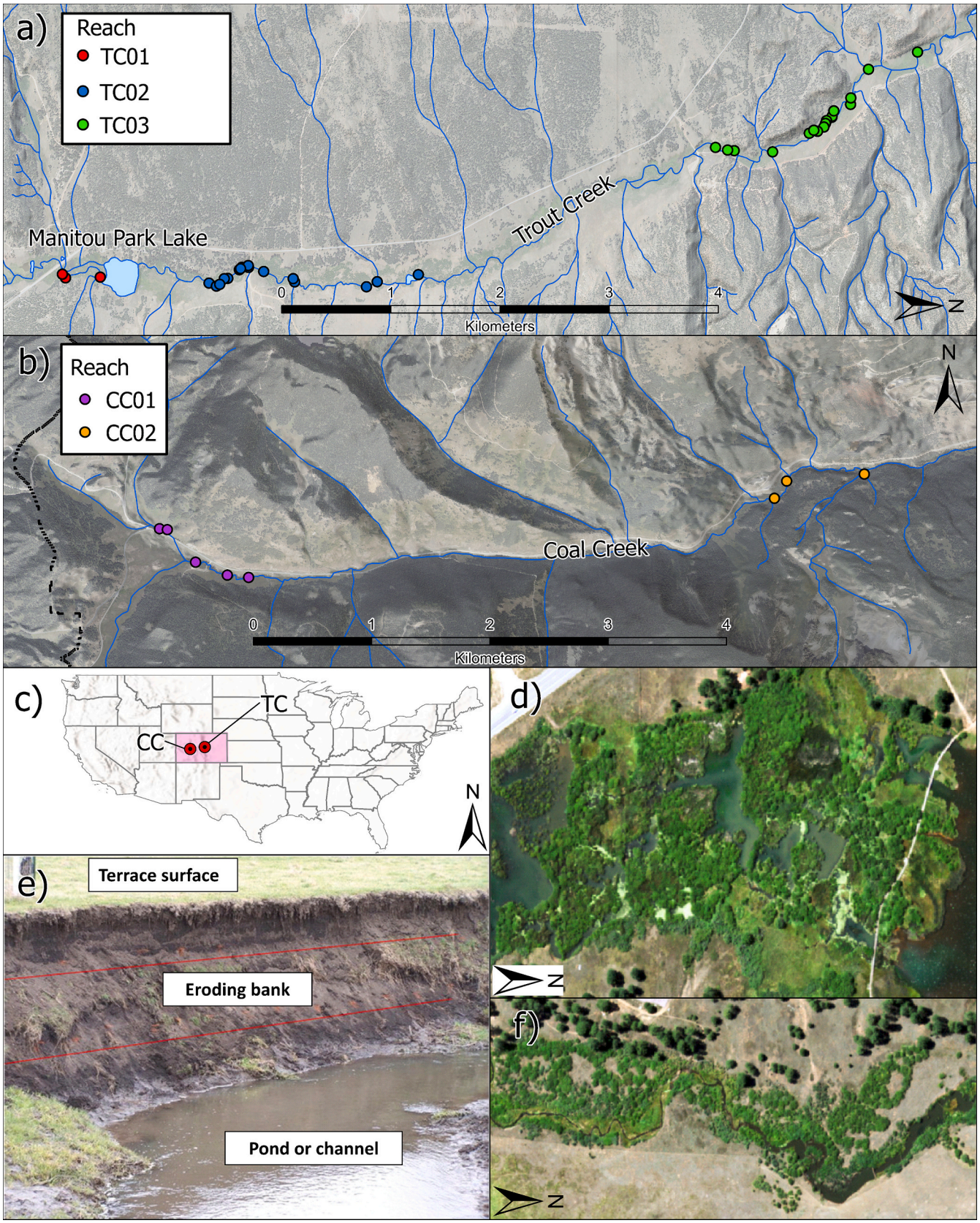

Fig. 1. Overview maps of (a) Trout Creek (TC) study area, (b) Coal Creek (CC) study area (points indicate surveyed beaver pond), (c) study areas shown within the state of Colorado (pink) and the contiguous USA, (d) aerial view of reach TC01, (e) image of high eroding bank within TC02, (f) aerial view of reach TC02. In (a), (b), (d), and (f), flow direction is from left (upstream) to right (downstream).

constructed in 1937 (USACE NID, 2022). TC01 has a wide riparian area with beaver pond cascades connected by a multi-threaded channel planform typical of a beaver meadow (Ives, 1942; Westbrook et al., 2011). Reaches TC02 and TC03 are downstream of the reservoir, and have a more incised, single-threaded channel planform (Fig. 1f) with high eroding banks (Fig. 1e). TC03 has some segments where the riparian area widens and a multi-threaded planform develops, but overall TC02 and TC03 exhibit lower lateral connectivity and narrower riparian areas compared to TC01.

Coal Creek, located in the Sawatch Range, is underlain primarily by Oligocene granodiorites of remnant laccoliths in the lower watershed and sedimentary rocks of the Eocene Wasatch Formation (feldspathic and arkosic sandstone, siltstone, and mudstone) and the Cretaceous Mesaverde Formation (various shales) in the upper watershed (Gaskill et al., 1987). The area has an average annual precipitation of 632 mm (USGS SNOTEL, 2023), and high flows occur in late spring and early summer due to snowmelt (USGS Gage Data, 2022). We conducted surveys of two reaches on Coal Creek. Reach CC01 is a wide, relatively low-gradient beaver meadow with numerous small anabranching channels. Reach CC02 has a narrower valley bottom compared to CC01; CC02 contains a well-defined main channel, although the adjacent floodplain hosts numerous side channels, beaver canals, and off-channel beaver ponds.

Both sites have a history of anthropogenic disturbance. Cattle grazing has occurred within the Trout Creek valley bottom since the late 1800's (Parker, 1937), and active cattle grazing was observed in the valley in TC02 during the 2022 field season. However, cattle are excluded from the riparian area by barbed wire fence in almost all other locations. During the 1990's or early 2000's, beaver were trapped along Trout Creek within the study area, reducing beaver populations, which is evident in historical aerial imagery (Alton, 2022; USGS EarthExplorer, 2021). Manitou Park Lake Dam has modified flows and sediment connectivity in TC02 and TC03 downstream of the dam, although the creek still experiences higher flows during spring snowmelt and during summer storms (USGS Gage Data, 2022). There are no significant dams, levees, or other anthropogenic features within or upstream of the Coal Creek study site, except for several small culverts and roads. However, there is a history of mining within the catchment that may affect sediment input and stream geochemistry (Ryan et al., 2009), and there was likely logging previously within the watershed.

2.2. Aerial photo analysis, estimations of beaver pond age, and pond selection

To estimate beaver pond age, which we used to calculate sedimentation and carbon accretion rates, we collected and analyzed aerial photos at both sites to develop a time series of beaver pond presence spanning from the early 1950's to 2021. Photo and image IDs are included in the supplementary material. We conducted field surveys in Summer 2022 to map beaver ponds along both creeks, estimating the age of the ponds from the historical aerial imagery. We defined a dam construction date as the midpoint between the timestamp of the earliest air photo in which the pond was identifiable and the timestamp of the preceding air photo. Pond ages were calculated as the difference between the 2022 survey date and the assumed dam construction date. We also calculated minimum and maximum possible pond ages using the bounding aerial photos to consider uncertainty in pond age. The largest difference between the best estimate for pond age and the minimum/maximum possible pond age was 1.71 years, except for one very old pond (> 66 years old), for which age constraints could not be established as it is visible in the earliest available aerial imagery in 1955.

2.3. Field data collection

We randomly selected ponds in which to conduct fieldwork from three age categories (old (> 9 years), medium (4–9 years old), and new (< 4 years old) selecting ponds from each age category within each reach, except when specific reaches lacked ponds of a certain age category. Additionally, we chose two cascades of ponds (one in TC02 and one in TC03) for sediment surveys. These cascades consisted of nine to ten adjacent ponds, allowing us to examine the influence of beaver pond cascades on sedimentation patterns. We surveyed a total of 45 selected ponds ($n = 3$ in TC01, $n = 14$ in TC02, $n = 19$ in TC03, $n = 6$ in CC01, and $n = 3$ in CC02). We also selected a few additional ponds from the old age category to sample for radiometric dating and analysis.

For sediment surveys, we adapted the V* sediment survey method (Butler and Malanson, 1995; Hilton and Lisle, 1993; Puttock et al., 2018; Scamardo and Wohl, 2020), sampling pond sediment depth using a sediment probe along a grid of points (Fig. A1). We also measured mean dam height using a meter tape, stadia rod, and level. Dam condition was classified visually as maintained, unmaintained, or unknown. Pond locations were classified as on-channel (referring to dams constructed on the main channel), off-channel, or deltaic (referring to ponds constructed where a channel flows into a reservoir). Additionally, we noted adjacent eroding high banks and measured their heights and lengths using a TruPulse laser rangefinder. Eroding high banks were observed exclusively in TC02 and TC03, and characterized by vertical, high (0.5–2 m), unvegetated banks along the outer bend of stream meanders where the stream was eroding into a higher terrace surface (Fig. 1e).

We determined OC content and grain size distribution of ponds by collecting short (< 40 cm) subaqueous cores or grab samples from each of the 45 ponds above the coarse alluvium layer. Short cores were collected to depth of resistance by inserting a universal sediment corer with a polycarbonate barrel (Aquatic Research Instruments, 2022). We also extracted long (30–130 cm) subaqueous cores for dating depth intervals from older beaver ponds via fallout radionuclides (FRNs). Suspended sediment samples were collected via Phillips samplers (Phillips et al., 2000) deployed for 25–30 days just upstream of sampled ponds along Trout Creek to establish initial activity concentrations of FRNs. All sediment samples were refrigerated at 4 °C immediately after collection. More detail on the process of extracting and extruding long cores, as well as suspended sediment sampling, is included in the supplementary material. To characterize the geomorphic characteristics of the reaches, we conducted surveys using an Emlid Reach RS2 RTK GPS (Emlid, 2022) for the Trout Creek study area, and relied on 1 m LiDAR derived digital elevation models (DEMs) for the Coal Creek study area due to limited field time (Breckheimer, 2019). Geomorphic data included slope, channel dimensions, trench width (the distance between terraces, or distance between steep hillslopes if terraces were not present), and trench depth (the depth from the surface of the terrace to the channel thalweg, or depth between highest floodplain surface to channel thalweg if terraces were not present). Full descriptions of geomorphic survey methods are included in the supplementary material.

2.4. Laboratory analyses

Sediment samples included long core sections taken for radiometric analysis and short cores and grab samples from ponds surveyed for grain size and OC analysis. We dried all samples at 105 °C for 24 h and sieved to <2 mm. For short cores and grab samples, we subsampled the <2 mm fraction (1–10 g) for analysis of OC content (% mass) via elemental analyzer at the CU Boulder Earth Systems Stable Isotope Laboratory (CUBES-SIL). OC stock and accretion rates were calculated from OC content, sediment bulk density, and pond age using equations reported in the supplementary material (Eqs. A1 and A2). We sent the remaining sediment from each short core/grab sample (50–150 g) to Ward Laboratories, where they were analyzed via hydrometer for % mass by grain size class (% clay, % silt, % sand). We sectioned long cores using depth increments between 1 and 4 cm depending on the volume of sediment needed (110 cm^3) for high-precision gamma spectrometry. Samples were sent to Fallout Radionuclide Analytics (FRNA) at Dartmouth College where they were analyzed via gamma spectrometry for ^{7}Be (half-

life = 53 days), ^{210}Pb (half-life = 22.3 years), and ^{137}Cs (half-life = 30 years). Subsamples analyzed for FRNs were also analyzed for grain size and OC content using the methods described above.

From deeper sediment within two long cores, we dated single pieces of woody organic material (twigs or small branches) using radiocarbon (^{14}C). We took both ^{14}C samples from sediment layers with a significant proportion of fine sediment, indicating lower velocity depositional conditions. The sediment layers in which the organic material were sampled from were also below coarser gravel layers that we interpreted as bed material load deposits. ^{14}C samples were dated using accelerator mass spectrometry (AMS) at Lawrence Livermore National Laboratory. Radiocarbon dates were reported in ^{14}C years for both samples. We calibrated the sample with a ^{14}C age of 110 years using the current internationally-ratified ^{14}C calibration curve (IntCal04) and the CALIB software program (Hua, 2009; Stuiver and Reimer, 1993). We calibrated the sample with a > modern result (indicating post-1950 material) using the CALIBomb software program and the 1955–2000 Northern Hemisphere Zone 1 calibration curve (Hua and Barbetti, 2004; Stuiver and Reimer, 1993).

2.5. Data analyses

To calculate R_{sed}, we employed two methods: 1) calculations based on the data collected from pond surveys and ages from aerial photos and 2) age models derived from FRN data. For (1), we determined R_{sed} for each pond by dividing the pond's D_{sed} by the pond's age. For (2), we used ^{7}Be and ^{210}Pb$_{xs}$ (excess ^{210}Pb) to establish a Linked Radionuclide Accumulation age model (LRC) for each core, since this approach accommodates non-steady state radionuclide input for sedimentation histories <150 years old (Landis et al., 2016). LRC age-depth models were created for two multidecade (10–100 years old) ponds at Trout Creek and three multidecade ponds at Coal Creek. We considered sediment at depths where ^{210}Pb$_{xs}$ approached zero to be old sediment (> 100 years old), corresponding to 5 half-lives of ^{210}Pb. In addition to LRC age-depth models, we used ^{14}C to calculate R_{sed} by dividing the calibrated ages by the sample depth. For both methods R_{sed} should be considered an integrated sedimentation rate, since it does not account for potential erosion/evacuation and re-deposition within ponds.

We conducted statistical analyses to assess correlations between R_{sed} (from pond surveys, not FRN data), D_{sed}, and OC content and potential controlling variables using Spearman correlation coefficients (ρ; for numerical variables) and Wilcoxon/Mann-Whitney tests and Kruskal-Wallis tests coupled with Dunn's tests (for categorical variables). We corrected for multiple comparisons using a Bonferroni correction. These tests included comparisons between study areas as well as between reaches within each study area. For all statistical analyses, we compared p-values to a significance level of $\alpha = 0.05$. P-values between 0.05 and 0.1 are also reported to assess weaker trends in the data.

2.6. Modeling channel infill using Monte Carlo simulations

To model the time needed for beaver pond sedimentation to infill incised channels, we conducted a Monte Carlo simulation using our sample distributions of pond longevities (the lifespan of ponds) and the fraction of time in which ponds present in 2021 were inundated between 2009 and 2021 (and thus accumulating sediment) using the Trout Creek aerial imagery dataset. We modeled the random construction of beaver dams (and vertical sediment accumulation over the life of the dam, based on Eq. (2)) within the most incised reach (TC02) and quantified the time needed (T_{infill}) to infill the channel to restore lateral connectivity with the terrace in TC02. In other words, we modeled the time required to reduce incision in TC02 so that it resembled TC01, which is not incised (conceptualized in Fig. 7a below). The number of iterations within the Monte Carlo simulation was increased by magnitudes of 10 until the mean T_{infill} varied <1 % over the course of repeated simulations, in this case 100,000 iterations (Oberle, 2015). Detailed methods related to simulated incised channel infill are given in the supplementary material.

3. Results

3.1. Beaver pond age and presence over time

The median pond age was 5.9 years at Trout Creek and 9.3 years at Coal Creek (Fig. 2a). Along Trout Creek, the number of beaver ponds visible from imagery was relatively low until increasing in the early 2000's, followed by a decrease between 2003 and 2009, then a steady increase from 2009 until the 2022 field season (Fig. 2b). TC02 had the largest variation in beaver pond number over time, while the number of beaver ponds in TC01 remained relatively stable from the 1950's until 2022 (Fig. 2b).

At CC01, we identified 15 beaver ponds in aerial imagery in 2012 and an additional 16 constructed between 2012 and 2022; none appeared to have breached within that time window, suggesting relatively stable dams (Google Earth, 2022; USGS EarthExplorer, 2021). Within CC02, we observed several dam breaches for on-channel ponds through imagery analyses and noted that most on-channel ponds visible in 2021 aerial imagery were no longer present during the 2022 field season (USGS EarthExplorer, 2021). Off-channel ponds in both CC01 and CC02 were some of the oldest ponds identified in this study.

3.2. Reach geomorphology

Overall, TC02 and TC03 have more incised channels, with a lower mean trench width:depth ratio than TC01 (Table 1). Channel geometry and trench depth (and thus trench width:depth ratio) could not be quantified for the CC study area due to the lack of field surveys, and TC01 did not contain a well-defined main channel but had a relatively wide trench width. In addition to being the most incised, we observed high eroding banks adjacent to sampled ponds in TC02 and TC03, being most prevalent in TC02. All ponds in TC02 and TC03 were located on the single main channel. CC02 had a narrower mean trench width than CC01, but contained secondary channels and off-channel ponds.

3.3. Sedimentation rates (R_{sed})

R_{sed} calculated from the pond survey/air photo method had a median of 6.2 cm yr^{-1} (mean = 12.7 cm yr^{-1}) and a median of 3.8 cm yr^{-1} (mean = 7.0 cm yr^{-1}) on Trout Creek and Coal Creek, respectively (Fig. 3a), but R_{sed} was not significantly different between study areas (Trout Creek versus Coal Creek; $p = 0.12$). When comparing reaches on Trout Creek, TC02 had a marginally higher R_{sed} than TC01 ($p = 0.08$), but no other significant differences in R_{sed} between reaches were observed ($p > 0.14$). R_{sed} was strongly negatively correlated with pond age at both Trout Creek ($\rho = -0.84$, $p < 0.01$; Fig. 3b) and Coal Creek ($\rho = -0.9$, $p < 0.01$; Fig. 3b). Similar to other studies, including Butler and Malanson (1995) and Pollock et al. (2007), R_{sed} can be related to pond age with a power equation, given below for Coal Creek (Eq. (1)) and Trout Creek (Eq. (2)) and shown in Fig. 3b and c:

$$R_{sed(Coal\ Creek)} = 13.0 \times Age_{pond}^{-0.60} \quad (1)$$

$$R_{sed(Trout\ Creek)} = 28.1 \times Age_{pond}^{-0.92} \quad (2)$$

with Age_{pond} as the estimated age of the pond from aerial imagery. However, it should be noted that pond age is included within both variables in the relationship, and thus some of this relationship may be spurious. Best fit power equations for minimum R_{sed} and maximum R_{sed}, calculated with the maximum and minimum pond age estimates from aerial photos, are also shown in Fig. 3b and c. Other relationships included a weak negative correlation between contributing watershed area (excluding the drainage area upstream of the dam) and R_{sed} at Trout

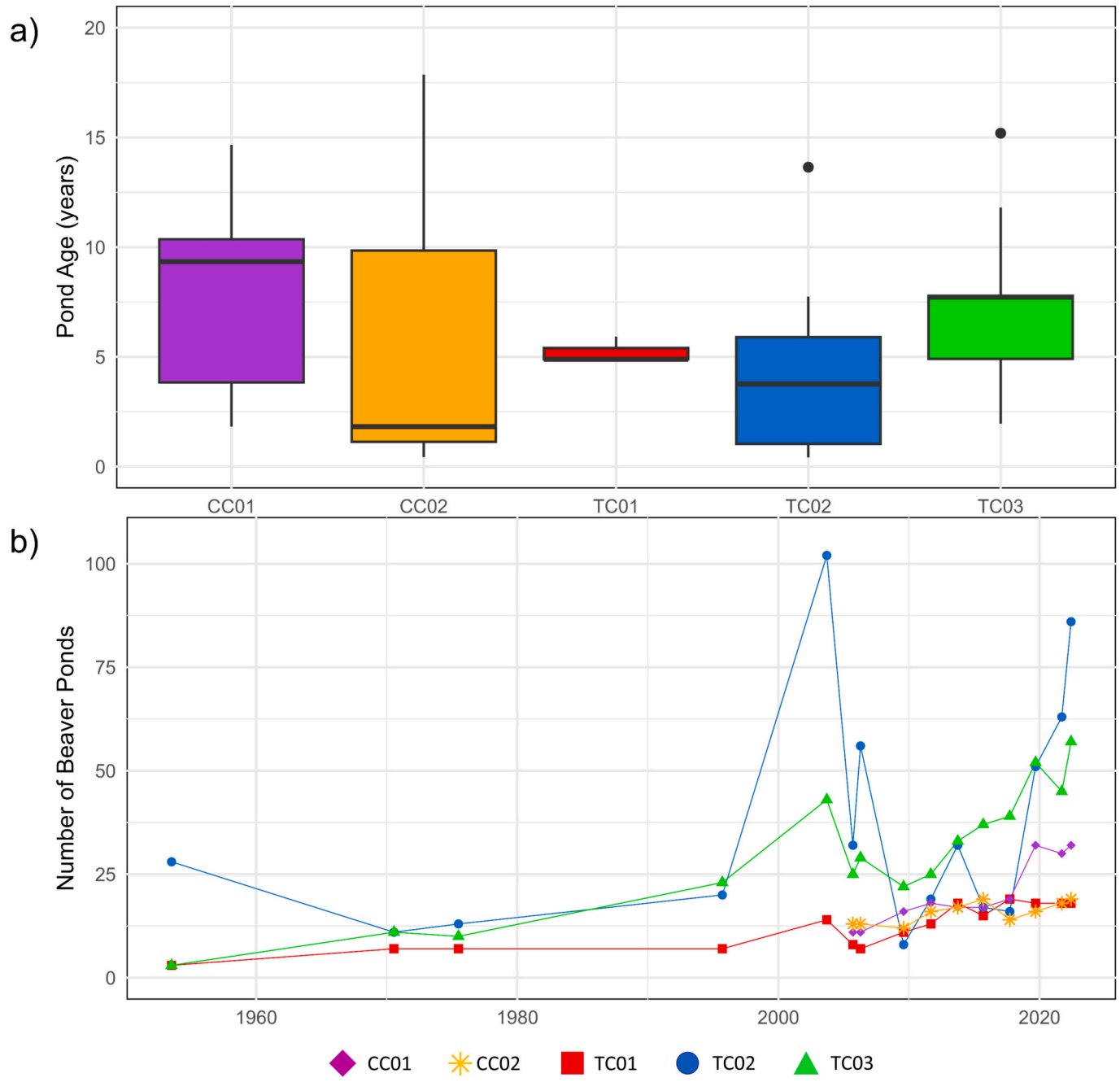

Fig. 2. (a) Distribution of estimated pond ages (includes 45 surveyed ponds) by reach, showing CC01 ($n = 6$), CC02 ($n = 3$), TC01 (n = 3), TC02 ($n = 16$), and TC03 ($n = 17$). CC01 includes a significant outlier (age = 66 years) not shown on plot, (b) number of all visible beaver ponds from 1953 to 2022 by reach.

Table 1
Geomorphic metrics calculated by reach.

Reach	TC01	TC02	TC03	CC01	CC02
Mean channel width (m)	N/A	21.69	9.28	N/A	N/A
Mean channel depth (m)	N/A	1.8	0.64	N/A	N/A
Mean channel W/D ratio	N/A	12.03	14.49	N/A	N/A
Mean trench width (m)	166.34	27.41	59.74	113.33	37.72
Mean trench depth (m)	0.82	2.15	1.01	N/A	N/A
Mean trench W/D ratio	207.55	12.91	74.53	N/A	N/A
Sinuosity	N/A	1.51	1.7	1.35	1.25
Mean slope (%)	N/A	0.68	0.57	1.91	1.67
Number of surveyed ponds with adjacent eroding banks	0	10	3	0	0
Contributing watershed area (km^2)	178.7	20	69.7	6.5	29.8

Creek ($\rho = -0.38$, $p = 0.02$; Fig. 3d), as well as a strong negative correlation between R_{sed} and mean dam height at Coal Creek only ($\rho = -0.84$, $p < 0.01$; Fig. 3e). We did not find significant downstream trends in R_{sed} within either of the two beaver pond cascades (Fig. A2a and A3a in the supplementary material). Spearman correlation coefficients and tests of significance between all numerical variables are reported in the supplementary material.

LRC age estimates demonstrated variations in R_{sed} with sediment depth and pond age. Depth profiles of grain size, OC content, FRN activity concentration, and LRC age calculations are shown for cores taken from Ponds #43 (~ 14 years old with aerial photo estimate; TC02; Fig. 4a, b, c, d, and e) and #226 (~37 years old with aerial photo estimate; TC03; Fig. 4f, g, h, i, j). LRC model age estimates for Pond #43 resulted in a R_{sed} of ~9 cm yr^{-1} for the top 11 cm of sediment when

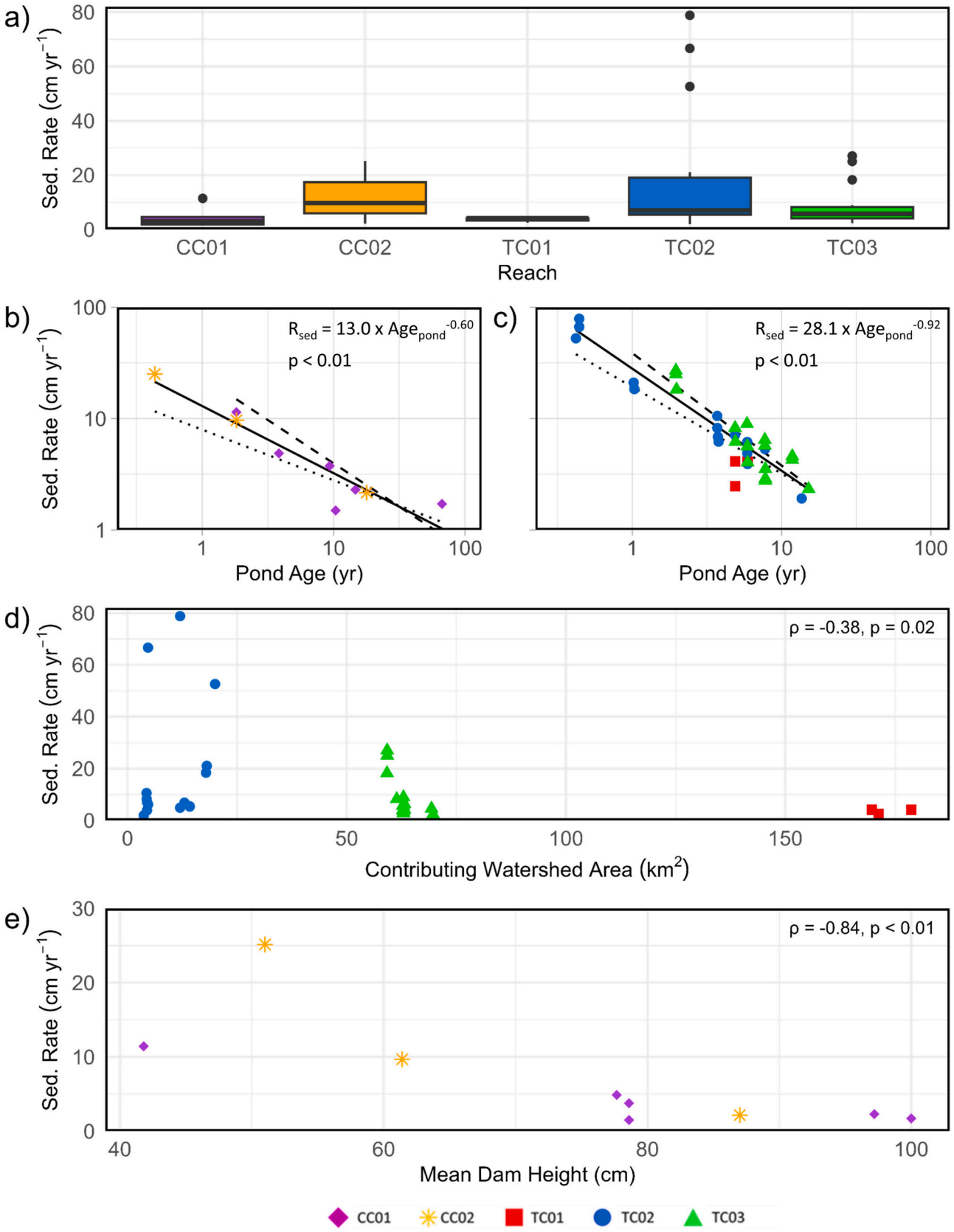

Fig. 3. R_{sed} in beaver ponds plotted (a) by reach, (b) versus pond age at Coal Creek, (c) versus pond age at Trout Creek, (d) versus contributing watershed area (excluding drainage area upstream of the impoundment) at Trout Creek, and (e) versus mean dam height at Coal Creek. For panels (b) and (c), note both axes are log transformed, with the best fit power equations shown by the black line and equation, and best fit power equations developed using minimum (dashed) and maximum (dotted) pond ages. Spearman's correlation coefficient (ρ) and *p*-values resulting from Spearman's rank sum tests are given where applicable.

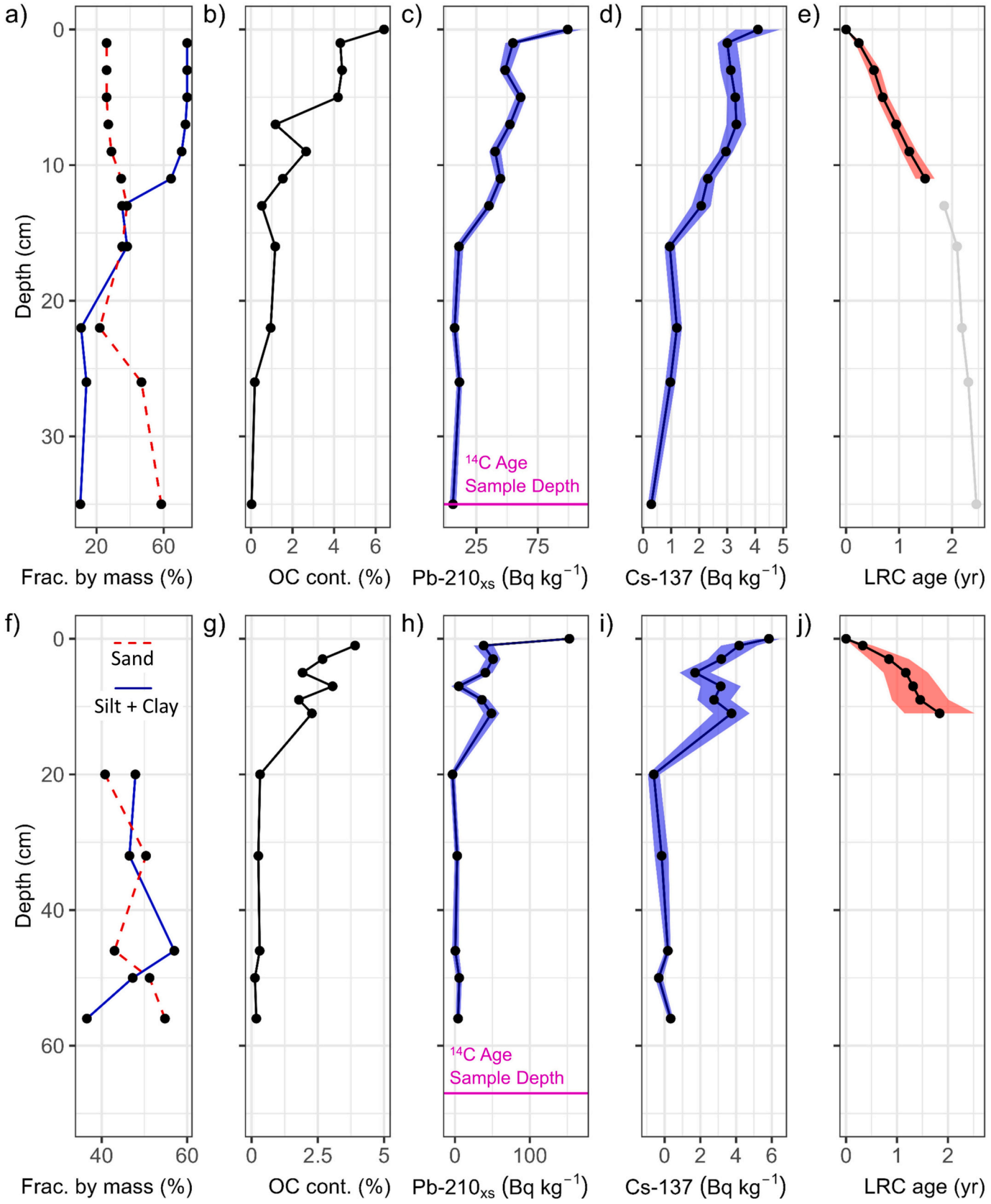

Fig. 4. Depth profiles for Pond #43 (panels a - e) and Pond #226 (panels f - j), showing (a,f) fraction by mass of fine sediment (clay + silt) and sand, (b, g) OC content, (c, h) $^{210}Pb_{xs}$ activity concentration, (d, i) ^{137}Cs activity concentration, and (e, j) LRC age estimates. Blue shading indicates 1 σ of uncertainty resulting from gamma spectroscopy measurements, while red shading indicates 2 σ. For (e), LRC age estimates shown in light gray should be taken with caution, as they likely underestimate true depositional age due to post-depositional migration of ^{7}Be radionuclides. For (f), lack of sufficient sample mass prevented grain size analysis of the top 6 samples. For (j), $^{210}Pb_{xs}$ activity concentrations were too low to apply LRC model below 12 cm.

applying the LRC model (Fig. 4e). Using the LRC model, Pond #226 had a R_{sed} of ~6 cm yr^{-1} for the top 11 cm of sediment (Fig. 4j). $^{210}Pb_{xs}$ and ^{137}Cs decay significantly by ~16 cm of depth at Pond #43 (Fig. 4c and d) and by ~20 cm of depth at Pond #226 (Fig. 4h and i). This indicates that deposited sediment below these depths likely predated the pond. Dated (^{14}C) organic material at 35 cm depth in Pond #43 resulted in calibrated 2σ age ranges of 1958 to 1993 CE, with the most probable age window between 1991 and 1993 CE (29–31 years old; probability = 0.869). Organic material at 67 cm depth in Pond #226 resulted in calibrated 2σ age ranges of 1684 to 1928 CE, with the most probable age window between 1803 and 1928 CE (94–219 years old; probability = 0.732). Dividing the minimum and maximum ages of the most probable calibrated age range by sample depths results in an integrated R_{sed} of 1.13–1.21 cm yr^{-1} and 0.31–0.71 cm yr^{-1} for Ponds #43 and #226, respectively. These calculations demonstrate that integrated R_{sed} calculated from FRNs align with predicted R_{sed} based on sediment probing (Eq. (2)). Integrated R_{sed} for the top 10–15 cm of these two ponds calculated from LRC age models and the R_{sed} for short term (< 5 year) ponds calculated via sediment probing (Fig. 3b and c) are on the order of magnitude of ~10 cm yr^{-1}. Integrated R_{sed} from ^{14}C ages are on the order of 0.1–1 cm yr^{-1}, also matching the expected R_{sed} at that depth as calculated via sediment probing (Fig. 3b and c). In both ponds, ^{14}C ages predate pond construction date as established via aerial photos. Finally, we applied the LRC age model to depths below where ^{7}Be was detectable (Fig. 4e), but the relatively young age estimates below this 12 cm depth are not reliable, as they do not align with older depositional age estimates from FRNs with longer half-lives (^{210}Pb, ^{137}Cs, and ^{14}C), nor the air photo record. Rather, these underestimated LRC ages at >12 cm depth likely result from post-depositional downward migration of ^{7}Be radionuclides. Additional long core depth profiles and details on ^{14}C dating are available in the supplementary material.

3.4. Mean fine sediment depth (D_{sed})

D_{sed} from pond surveys had a median of 31.9 cm (mean = 33.6 cm) and a median of 20.8 cm (mean = 34.0 cm) on Trout Creek and Coal Creek, respectively (Fig. 5a). There were no significant differences in D_{sed} when comparing D_{sed} between study areas (Trout Creek versus Coal Creek; $p = 0.11$). Comparisons among reaches on Trout Creek indicated that D_{sed} in TC01 is significantly lower than that of TC03 ($p < 0.01$), and TC02 ($p = 0.02$). D_{sed} was positively correlated with pond surface area at Trout Creek ($\rho = 0.35$, $p = 0.04$; Fig. 5b). For Coal Creek, D_{sed} was strongly positively correlated with pond age ($\rho = 0.75$, $p = 0.03$; Fig. 5c), but this relationship was not present for Trout Creek. D_{sed} was also moderately positively correlated with mean dam height at Coal Creek ($\rho = 0.69$, $p = 0.04$; Fig. 5d). When examining additional relationships between variables, we found correlation between the volumetric fraction of beaver pond filled with fine sediment (V*) and the pond age on Trout Creek ($\rho = 0.36$, $p = 0.03$; Fig. 5f) and on Coal Creek ($\rho = 0.73$, $p = 0.02$; Fig. 5e), indicating ponds filling to their max storage capacity over time. We also found a strong positive correlation between mean dam height and pond age at Coal Creek ($\rho = 0.96$, $p < 0.01$). No significant downstream trends in D_{sed} were observed within either of the two beaver pond cascades (see Fig. A2b and A3b).

3.5. OC content, stock, and accretion rate

Sediment OC content in ponds had a median of 0.8 % (mean = 1.3 %) and a median of 1.7 % (mean = 3.0 %) for Trout Creek and Coal Creek, respectively, with the highest OC content in CC01 (Fig. 6a). Within Coal Creek, OC content was higher (marginal significance) in CC01 compared to CC02 ($p = 0.09$). No other significant differences were found when comparing between the two study areas or among reaches on Trout Creek ($p > 0.2$ for all comparisons). Fraction fine sediment (clay + silt) by mass was positively correlated with OC content within beaver ponds at both Coal Creek ($\rho = 0.83$, $p < 0.01$; Fig. 6b) and Trout Creek ($\rho = 0.79$, $p < 0.01$; Fig. 6c). Within the TC03 cascade, there was a strong negative correlation between distance downstream and OC content ($\rho = -0.80$, $p = 0.01$; Fig. A3d); there was no correlation between distance downstream and OC content for the TC02 cascade ($\rho = -0.40$, $p = 0.29$; Fig. A2d). At Coal Creek, contributing watershed area was negatively correlated with OC content ($\rho = -0.68$, $p = 0.04$; Fig. 6d), and D_{sed} was positively correlated with OC content ($\rho = 0.70$, $p = 0.04$; Fig. 6e).

Mean OC stock was 17.4 Mg ha^{-1} (1740 g m^{-2}) within Trout Creek beaver ponds and 28.8 Mg ha^{-1} (2880 g m^{-2}) within Coal Creek beaver ponds (Fig. A7). Note that these stock calculations are for variable depths since the mean depth of fine sediment of each beaver pond was used to compute stocks. OC accretion rates had a median of 3.8 Mg ha^{-1} yr^{-1} (380 g m^{-2} yr^{-1}) within the Trout Creek study area and a median of 5.6 Mg ha^{-1} yr^{-1} (560 g m^{-2} yr^{-1}) within the Coal Creek study area (Fig. 6f). When comparing reaches on Trout Creek, both OC stock and OC accretion rate were significantly lower in TC01 than in TC03 ($p = 0.02$, $p = 0.03$, respectively; Fig. 6f). CC01 had the highest calculated OC stock and OC accretion rate of any of the reaches, but comparisons between CC01 and CC02 were not included due to small sample size for CC02 ($n = 1$ for OC analyses).

Activity concentrations of FRNs, OC content, and grain size appear to be associated, as activity concentrations and OC content closely track grain size variations (Fig. 4). Even in older, deeper sediment, OC content can remain relatively high if the sediment has a high fraction of fines, as was most evident in Pond #46 (see Fig. A4a and A4b). However, this was not always the case; for example, Pond #226 contained high fraction fines at depth (e.g., at 46 cm) but had low OC content (Fig. 4g and h). Coarse sediment samples were very low in OC and FRN activity in all cases.

3.6. Time required to re-connect incised channel to terrace

We used mean geomorphic characteristics of TC02 and TC01 (Table 1; Fig. 7a) to determine D_{infill}, the depth required to reconnect the TC02 channel to the terrace within the river corridor and approximate TC01 morphology. D_{infill} is equal to the mean trench depth of TC02 (2.15 m) minus the mean trench depth of TC01 (0.82 m), resulting in a D_{infill} of 1.33 m. Aerial photo analysis of TC02 indicated that between 2009 and 2021, the median fraction of time inundated for the ponds present in 2021 ($n = 77$) was approximately 28.6 % of the time window analyzed. We also found that the median longevity of ponds in TC02 calculated using the entire record of aerial imagery for TC02 was 4.00 years. The median longevity of the full inventory of ponds for TC02 (4.00 years) was likely longer than the median pond age of surveyed ponds for TC02 (3.76 years) because the surveyed pond selection was a smaller sample size and is made up entirely of ponds that have not been abandoned and thus not reached their maximum age. From the 100,000 iterations, the median time needed (T_{infill}) to infill the most incised (TC02) channel to reconnect the terrace and achieve TC01 trench geometry was 96.2 years, with a minimum of 19.8 years, first quartile of 72.3 years, 3rd quartile of 132.0 years, and maximum of 697.7 years (Fig. 7b). Mean T_{infill} was 110.9 years, with a standard deviation of 58.5 years. Dividing D_{infill} by the modeled median T_{infill} results in a long-term (~100 years) R_{sed} of 1.4 cm yr^{-1}.

4. Discussion

4.1. Controls on sedimentation in beaver ponds

We found that the integrated R_{sed} declines with pond age according to a power equation (Eqs. (1) and (2); Fig. 3b and c), similar to power relationships developed for beaver pond age and R_{sed} the northern Rocky Mountains (Butler and Malanson, 1995) and in the high desert in eastern Oregon, USA (Pollock et al., 2007). Our pond survey and LRC age model results indicate that following dam construction, beaver ponds rapidly aggregated sediment on the scale of 10 cm yr^{-1} for ~1–3 years. If an

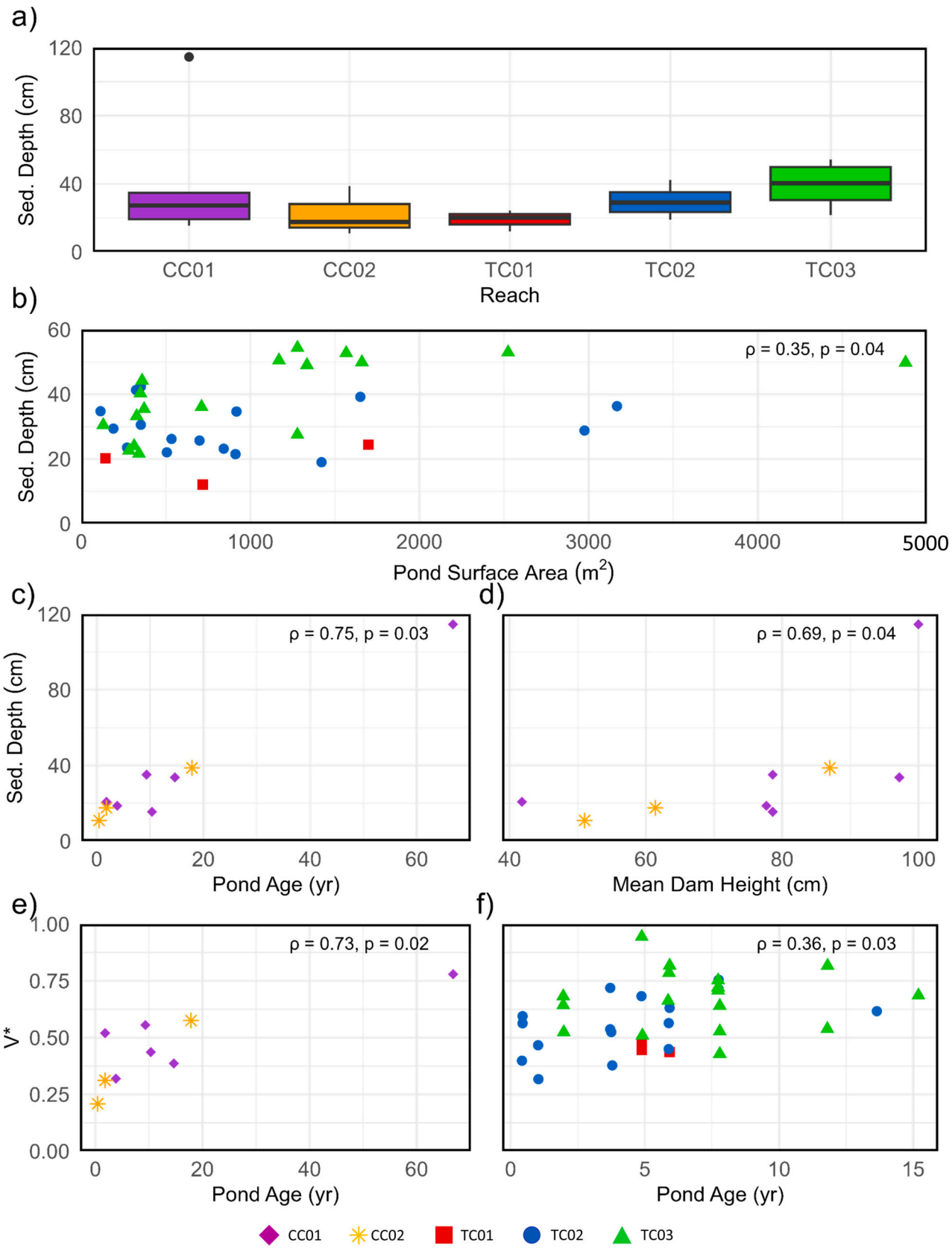

Fig. 5. D_{sed} in beaver ponds plotted (a) by reach, (b) versus pond surface area at Trout Creek, (c) versus pond age at Coal Creek, (d) versus mean dam height at Coal Creek. V* versus pond age is plotted for (e) Coal Creek and (f) Trout Creek. ρ and *p*-values resulting from Spearman's rank sum tests are given where applicable.

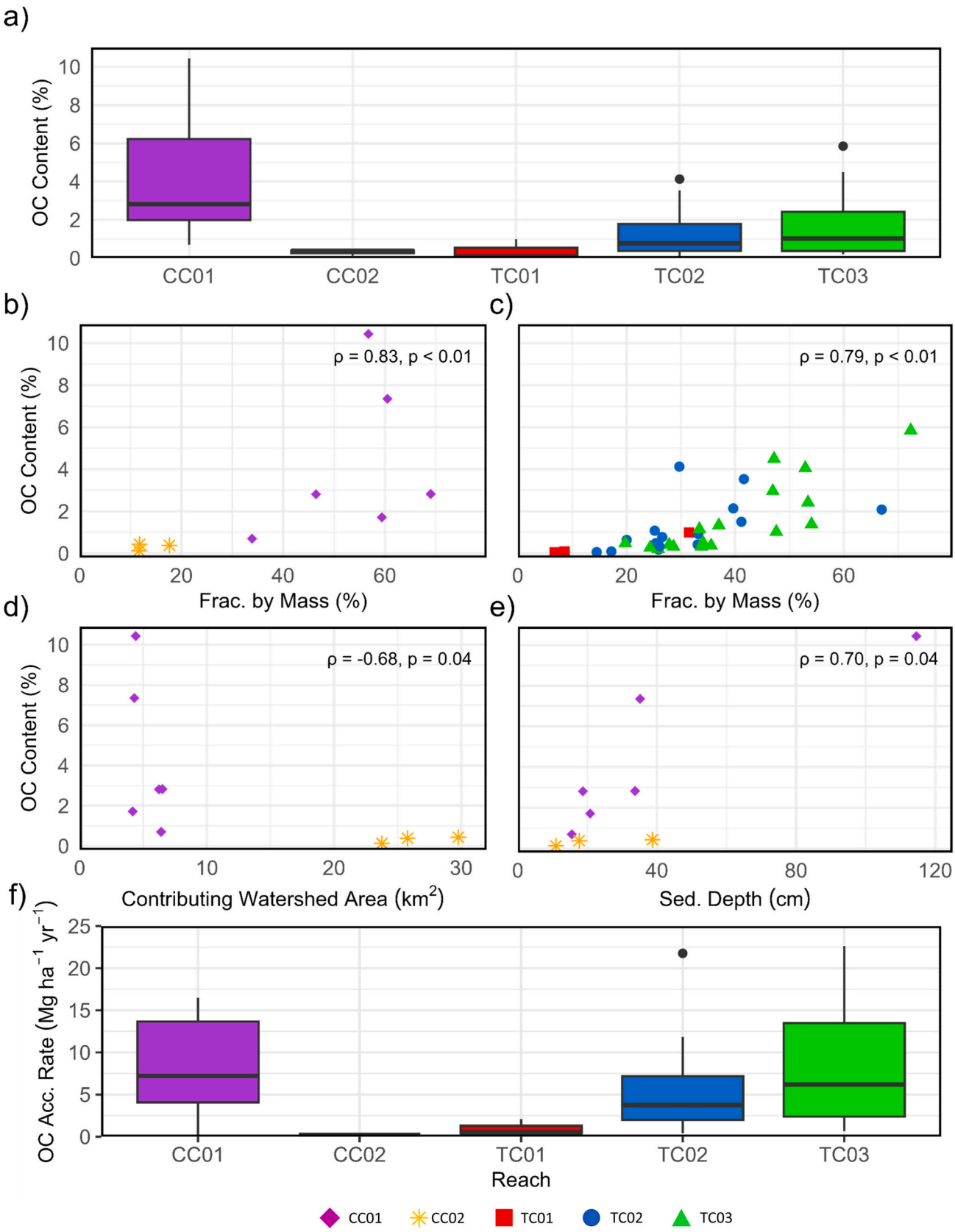

Fig. 6. OC content in beaver pond sediment (a) by reach, (b) versus fraction by mass of fine sediment (silt + clay) at Coal Creek, (c) versus fraction by mass of fine sediment at Trout Creek, (d) versus contributing watershed area at Coal Creek, (e) versus D_{sed} at Coal Creek. (f) shows sediment OC accretion rate by reach. ρ and p-values resulting from Spearman's rank sum tests are given where applicable.

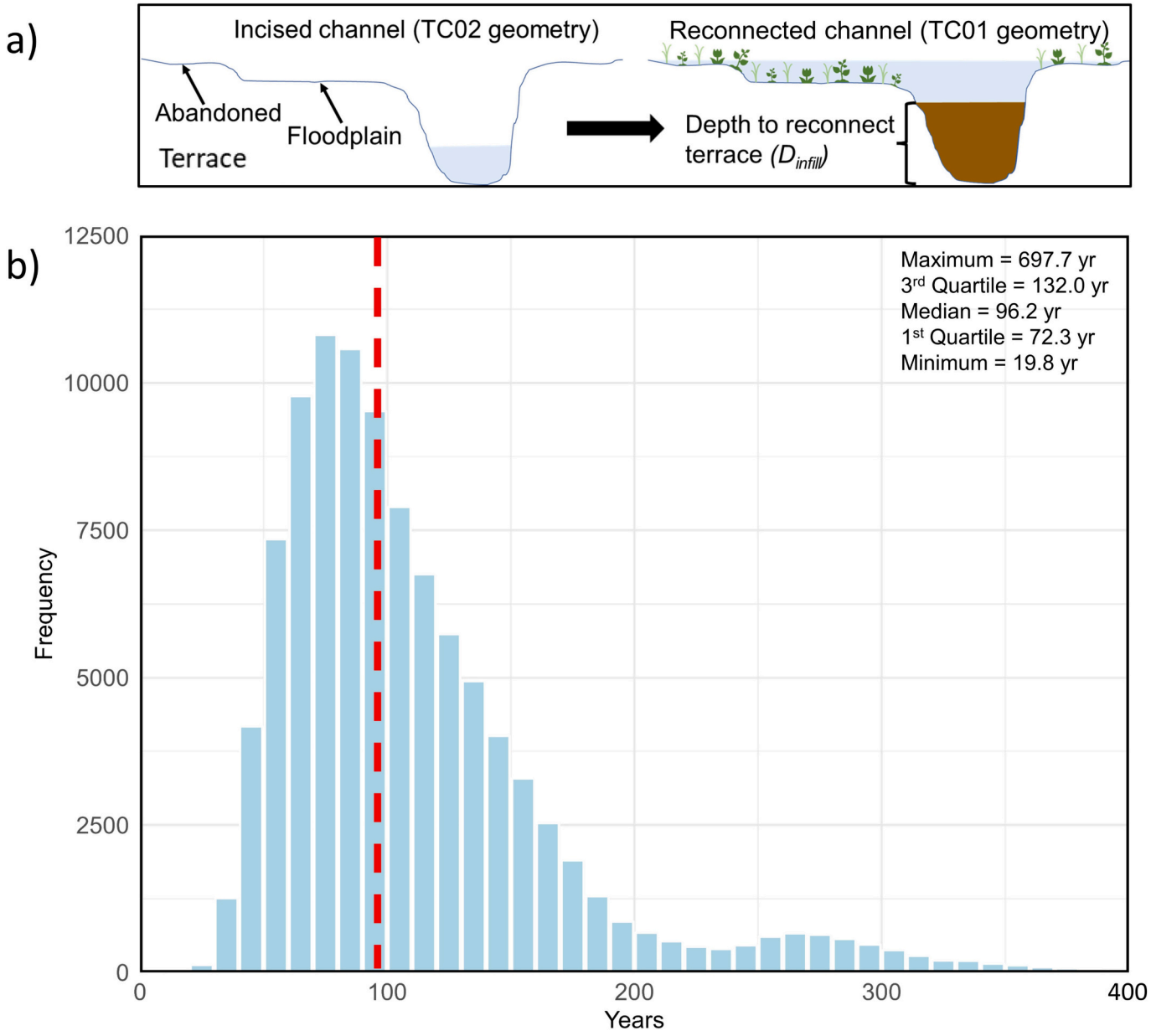

Fig. 7. (a) Diagram depicting the infill of an incised stream (approximated using TC02 trench geometry) via sedimentation of D_{infill} (shown in brown), to a laterally reconnected (between channel and floodplain) stream (approximated using TC01 trench geometry). (b) Frequency distribution of T_{infill} for Monte Carlo simulations, with median T_{infill} (96.2 years) shown by the vertical red dashed line.

individual beaver pond remains inundated past these initial few years, the integrated R_{sed} over the time the pond exists decreased, as is evident from surveys of older ponds and ^{14}C ages. The decline in R_{sed} is likely due to multiple factors, including ponds reaching sediment storage capacity. With an increase in V* (the fraction of the ponds volume filled with sediment) (Fig. 5e and f), ponds may be abandoned by beaver after a few years (Levine and Meyer, 2014), although beaver can also inhabit ponds for longer periods of time (James and Lanman, 2012; Johnston, 2015). Abandonment may result in unmaintained dams that are less effective at sediment retention and reduced beaver activity promoting sedimentation (e.g., burrowing, construction, etc.). Previous studies that have found that a significant portion (up to 30 %) of sediment and organic inputs in active beaver ponds are a product of beaver activity such as burrow construction, canal excavation, and woody material storage (Hood and Larson, 2015; McCreesh et al., 2019; Puttock et al., 2018), thus older, abandoned beaver ponds may have lower overall sedimentation rates.

In addition to reaching sediment storage capacity and potential beaver abandonment, our study indicates that differences in geomorphic context (i.e., incision and valley geometry) also likely influenced the relationship between R_{sed} and pond age. Our study reaches included both single thread, relatively incised channels as well as multi-thread beaver meadows, and the relationship between R_{sed} and D_{sed} and pond age differed somewhat between these two types of reaches. R_{sed} and radionuclide ages from the incised reaches (TC02 and TC03) downstream of the dam on Trout Creek indicate that ponds likely scour and fill episodically, resulting in a lower integrated R_{sed} as ponds age. These reaches have a relatively narrow, deep trench and a well-defined main channel, potentially increasing stream power and resulting in dam breaching during higher-flow events. Dam breaches and dam rebuilding also likely promote episodic erosion and deposition (Butler and Malanson, 2005; Levine and Meyer, 2014; Pearce et al., 2021; Pollock et al., 2014), and thus over time integrated R_{sed} is lower for older ponds.

The inferred age discontinuity in FRN age data supports that episodic

sedimentation and erosion (i.e., fill and scour) are occurring within beaver ponds in TC02 and TC03. Additionally, ^{14}C dated organic samples were both from layers with a high fraction of fine sediment, below a coarser layer that we interpreted as bed material load deposits. Thus, the fine layers in which ^{14}C samples were taken could indicate a previous period of ponding, either via beaver or another mechanism. These results point to the presence of an older "storage" layer below a 10–20 cm thick "active" layer of recently accumulated fine sediment from the construction of beaver dams and episodic scour and fill. Assuming there are similar active and storage layers within ponds of all ages, there would be a relatively random D_{sed} regardless of pond age (as observed on Trout Creek), and an upper limit on D_{sed} accumulation within beaver ponds on the scale of 10–100 cm, which was the range of D_{sed} within our dataset. Thus, with increasing pond age, integrated R_{sed} would decrease substantially.

Although episodic scour and fill is likely occurring to some degree across all the study reaches, data from the reaches on Coal Creek and from TC01 indicate that ponds in multi-thread reaches with wider active floodplains (i.e., greater trench width) likely experience more continuous sedimentation, even within ponds >10 years old. CC01 and TC01 are multi-thread beaver meadows, and CC02 hosted numerous side-channels and off-channel beaver ponds. These geomorphic settings, which are likely lower energy environments compared to incised single thread reaches (like TC02), likely result in less scour of pond sediment. Evidence for this includes the observed increase in D_{sed} with increasing pond age at Coal Creek, as one might expect to occur without significant and frequent scour and fill (Fig. 5c). In addition, R_{sed} at Coal Creek decays less rapidly with increasing pond age than at Trout Creek, as seen by the less negative exponent within Eq. (1) when compared to the exponent in Eq. (2). On Coal Creek, we also observed beaver dam height increased with pond age, indicating that beaver may be adding material to dams; as a result, we found higher D_{sed} in ponds with greater dam height (Fig. 5d). The increase in dam height and D_{sed} with pond age at Coal Creek aligns with previous research indicating that if dams remain stable and intact, beaver may add to their total height, leading to greater total sediment storage (Meentemeyer and Butler, 1999; de Visscher et al., 2014). Our results indicate that for sediment stored in beaver dams to persist, there may need to be accommodation space within the valley bottom for the creation of low energy, multi-thread beaver meadows, or for beaver to create ponds on side channels (Levine and Meyer, 2014; Polvi and Wohl, 2012). More work is needed to determine under which conditions beaver ponds are more likely to experience continuous sedimentation as opposed to scour and fill dynamics.

Additional results contribute to further understanding of how beaver influence sedimentation in river corridors. For example, we did not find any downstream trends R_{sed} or D_{sed} within beaver pond cascades in TC02 and TC03 (Fig. A2 and A3), similar to results from other beaver pond sequences such as those in the forested Ardennes region in Belgium (de Visscher et al., 2014). The lack of trends in cascades may be a result of downstream ponds receiving pulses of sediment from upstream dam failures (Bigler et al., 2001; Levine and Meyer, 2014; Puttock et al., 2018; de Visscher et al., 2014). Also similar to other studies, we also observed that Trout Creek ponds with larger surface area had higher D_{sed} (Fig. 5b), which may result from lower incoming flow velocities in larger ponds enhancing sediment deposition (John and Klein, 2004; de Visscher et al., 2014; Giriat et al., 2016; Puttock et al., 2018).

Our results demonstrate that both short-term and multidecade vertical sedimentation rates in beaver ponds within headwater catchments in the southern Rocky Mountains are comparable to those from different climates and topographies (see Table A6 in the supplementary material). Larsen et al. (2021) noted studies of beaver ponds within montane watersheds tended to have higher R_{sed} (typically >10 cm yr^{-1}) than those from lowland watersheds (typically <10 cm yr^{-1}). This could be due to montane watersheds having higher rates of sediment production and supply (Milliman and Syvitski, 1992). Mean R_{sed} at our study sites in the southern Rocky Mountains fall between published rates in lowland and montane watersheds, which may in part be due to lower sediment production in our drainage areas due to weathering-resistant granitic lithology, particularly at Trout Creek. Additionally, because this study includes a larger proportion of older ponds, the mean R_{sed} is likely slightly lower than previous studies in mountainous environments that focused only on very young ponds, as R_{sed} decreases with pond age (Fig. 3b and c).

R_{sed} from our study are similar to rates calculated from ponds constructed by the Eurasian beaver (*castor fiber*; Table A6). Previous studies have suggested that the *castor fiber* tend to build less dams and smaller dams than *castor canadensis*, and that *castor canadensis* colonize streams faster, are slightly larger than *castor fiber*, and may outcompete *castor fiber* when occupying the same area (Gurnell, 1998). When comparing R_{sed} between ponds constructed by *castor canadensis* and *castor fiber*, we see that local, reach-scale, and watershed scale variables seem to exert more control over R_{sed} and pond longevity than interspecies variability (Table A6). R_{sed} within beaver ponds constructed by *castor fiber* in Eurasia range from 2.9 to 14 cm yr^{-1} (Giriat et al., 2016; John and Klein, 2004; Puttock et al., 2018; de Visscher et al., 2014), compared to 0.25–79 cm yr^{-1} within ponds constructed by *castor canadensis* (Butler and Malanson, 2005, 1995; Devito and Dillon, 1993; Pollock et al., 2007; this study). Although there appears to be greater variability within R_{sed} in North American ponds, the age range of these ponds is greater as well.

4.2. Beaver promote OC accretion due to pond sedimentation

Our study adds to knowledge of how beaver impact OC storage and dynamics within river corridors. Similar to previous studies in river corridors, grain size was strongly correlated with OC content (Fig. 6b and c) (Lininger et al., 2018; Scott and Wohl, 2018; Sutfin et al., 2021; Westbrook et al., 2011). Although the oldest pond in this study (Pond #15; CC01 ~ 66 years old) had the highest sediment OC content (9–29 %) of any pond in the study (Fig. A6a), OC content was not correlated with pond age at either study site, in contrast to previous studies which found older ponds to contain higher sediment OC content (Butler and Malanson, 1995; Murray et al., 2021). Further work is needed to tease out controls on OC content within beaver pond sediment. Overall, OC content in beaver pond sediment at our study sites, particularly at Trout Creek, was lower compared to similar studies (Table A7). However, in these studies, the sediment samples generally had finer grain size distributions than those in our study (Butler and Malanson, 1995; Murray et al., 2021; Westbrook et al., 2011).

By combining sedimentation rates with OC content, we estimated OC accretion rates in the beaver ponds on Trout Creek and Coal Creek, which has seldom been reported in previous studies. Although OC accretion rates had a wide range (0.13 to 22.6 Mg ha^{-1} yr^{-1}) beaver ponds accumulate OC more rapidly than previously published rates within floodplains (Sutfin et al., 2016), indicating that sedimentation in beaver ponds may be an important process in river corridor OC dynamics. Previous studies have shown that beaver can increase methane emissions due to ponding (Cazzolla Gatti et al., 2018; Nummi et al., 2018; Weyhenmeyer, 1999), but to determine the net effect of beaver on OC dynamics, we must incorporate all fluxes, including OC accretion in sediment. Whether OC associated with sediment in beaver ponds persists is dependent on the fate of the sediment and rates of decomposition, but we found cases of high OC content in deeper fine sediment layers. These deposits may indicate previous beaver ponds or slack water deposits (Kramer et al., 2012; Persico and Meyer, 2009; Polvi and Wohl, 2012), but further work is needed to determine whether the deposits were a result of beaver activity. Higher OC content in deeper sediment in some of the studied ponds at Trout Creek supports previous work indicating that relict beaver meadows can store substantial OC stocks decades after abandonment (Laurel and Wohl, 2019).

4.3. Modeling beaver-related channel-floodplain reconnection

Monte Carlo simulations indicated that it takes a relatively long time (median = 96.2 years) for stochastic construction of beaver dams and their persistence to transform the most incised reach (TC02) to a state resembling TC01 geometry (a beaver meadow) (Fig. 7b). Using the median time for infill from the simulations and the 1.33 D_{infill} required results in an estimated 1.4 cm yr^{-1} aggradation rate, which is lower (albeit the same order of magnitude) than rates of beaver-assisted channel infill from Beechie et al. (2008) and Pollock et al. (2007), who used single channel infill rates of 3 cm yr^{-1} and 5 cm yr^{-1}, respectively. However, the Monte Carlo simulation approach used in this study expands on these previous estimates because we considered different R_{sed} depending on pond age, and variations in pond persistence on longevity, resulting in a distribution of T_{infill} as opposed to assuming average rates. Using the aerial imagery record, we found that the fraction of time locations were not inundated can be relatively large, and the large field dataset of R_{sed} contained significant variation between ponds (Fig. 3). Our results indicated that estimating the timescale of reversing channel incision via beaver activity should account for both spatial and temporal variability.

Our simulations of incised channel infill relied on several assumptions, the first of which was that age was the only predictor of R_{sed}. Thus, we ignored variations in pond geometry or other factors when modeling pond sedimentation. In addition, we did not explicitly model sediment evacuation/erosion in the case of beaver dam failure, which has been observed in other field studies (Butler and Malanson, 2005; Levine and Meyer, 2014; Pearce et al., 2021) and is indicated by our radiometric dating. Despite this, our equations for integrated R_{sed} included older ponds, meaning that the calculated R_{sed} included any scour and fill episodes. Future work could include explicit consideration of scouring and post breach erosion. We also assumed that the density of beaver ponds on Trout Creek between 2009 and 2021 (the time window used to develop our distribution of fraction of time inundated) is the closest approximation to the intensity of beaver activity and pond construction that might occur on Trout Creek given continuous beaver activity unimpeded by human activities. Finally, although we considered the time in which a pond location was not inundated and thus was not accumulating sediment, we did not account for the potential for channel avulsion and pond abandonment that might preserve deposited sediment. Thus, future modeling efforts could expand the spatial and temporal complexity of simulation by including sedimentation dynamics within ponds on adjacent side-channels and floodplains and on decadal and centennial timescales, to model how beaver activity affects the longer-term geomorphic evolution of the river corridor.

Management approaches aimed at restoring incised streams have emphasized sediment retention structures, including natural beaver dams, beaver dam analogues (BDAs), and other introduced wood and earthen structures meant to restore natural stream processes and form (Pollock et al., 2014; Davis et al., 2021; Norman et al., 2022; Pearce et al., 2021; Yarnell et al., 2020). Process-based stream restoration practices have made efforts to consider larger spatial extents and longer temporal scales when restoring river corridors, and thus require an understanding of how different processes influence sediment and OC retention across scales (Beechie et al., 2010). The modeling of incised channel infill using Monte Carlo simulations demonstrated that restoring incised channels to increase channel-floodplain connectivity may likely take 100 years or more, significantly longer than the timelines of many ongoing and planned restoration projects (Yarnell et al., 2020), which should be considered by restoration practitioners.

5. Conclusion

Using sediment surveys of a large dataset of ponds situated in differing geomorphic contexts coupled with historical air photo analyses and radiometric dating, we found that R_{sed} decreases non-linearly with pond age. Within incised reaches in this study, we found evidence of scour and fill dynamics in main channel ponds. This contrasts with less-incised reaches, where we found that although R_{sed} similarly decreased with pond age, the ponds were likely more stable and D_{sed} and dam heights increased with pond age. In addition, grain size was strongly correlated with OC content of pond sediment, and OC accretion rates due to pond sedimentation can be relatively high. Finally, Monte Carlo simulations estimated that beaver pond-related sedimentation could reduce incision and promote channel-floodplain connectivity on the timescale of ~100 years. Our work provides insight into R_{sed}, D_{sed}, and OC content and stock using a large sample size of beaver ponds ($n = 45$) that spanned pond ages compared to previous studies. This research can inform future efforts at beaver-based restoration and provides insight into spatial and temporal dynamics of sediment and OC within beaver mediated river corridors.

CRediT authorship contribution statement

J.C. Rees: Writing – review & editing, Writing – original draft, Visualization, Validation, Resources, Methodology, Investigation, Funding acquisition, Formal analysis, Data curation, Conceptualization. **K.B. Lininger:** Writing – review & editing, Supervision, Methodology, Investigation. **J.D. Landis:** Validation, Supervision, Resources, Investigation, Formal analysis, Data curation. **C.E. Briles:** Writing – review & editing, Resources, Methodology, Conceptualization.

Declaration of competing interest

The authors declare that they have no known competing financial interests or personal relationships that could have appeared to influence the work reported in this paper.

Data availability

Data are publicly available on Hydroshare at https://www.hydroshare.org/resource/c9bf926f707e4d4ab9763b93acf81a0e/.

Acknowledgements

We thank Professors Holly Barnard and Katie Snell for comments on an initial version of this manuscript. Funding was provided by the CU Boulder Geography Department, the Rocky Mountain Biological Laboratory, and the National Science Foundation [Award #2012669 "Collaborative Research: Network Cluster: Quantifying controls and feedbacks of dynamic storage on critical zone processes in western montane watersheds"]. We acknowledge the analytical contributions of the CU Boulder Earth Systems Stable Isotope Lab (CUBES-SIL) Core Facility (RRID:SCR_019300), Fallout Radionuclide Analytics (FRNA) at Dartmouth College, and the Center for Accelerator Mass Spectrometry (CAMS) at Lawrence Livermore National Laboratory (LLNL).

Appendix A. Supplementary data

Supplementary data to this article can be found online at https://doi.org/10.1016/j.scitotenv.2024.174951.

References

Adams, M.B., Loughry, L., Plaugher . comps, L., 2008. Experimental Forests and Ranges of the USDA Forest Service, No. NE-GTR-321. U.S. Department of Agriculture, Forest Service, Northeastern Research Station, Newtown Square, PA. https://doi.org/10.2737/NE-GTR-321.

Alton, S.K., 2022. USFS Manitou Experimental Forest Manager. Personal Communication.

Aquatic Research Instruments, 2022. The Universal Corer. URL. http://www.aquaticresearch.com/ (accessed 4.19.2022).

Beechie, T.J., Pollock, M.M., Baker, S., 2008. Channel incision, evolution and potential recovery in the Walla Walla and Tucannon River basins, northwestern USA. Earth Surf. Process. Landf. 33, 784–800. https://doi.org/10.1002/esp.1578.
Beechie, T.J., Sear, D.A., Olden, J.D., Pess, G.R., Buffington, J.M., Moir, H., Roni, P., Pollock, M.M., 2010. Process-based principles for Restoring River ecosystems. BioScience 60, 209–222. https://doi.org/10.1525/bio.2010.60.3.7.
Bigler, W., Butler, D.R., Dixon, R.W., 2001. Beaver-pond sequence morphology and sedimentation in northwestern Montana. Phys. Geogr. 22, 531–540. https://doi.org/10.1080/02723646.2001.10642758.
Brazier, R.E., Puttock, A., Graham, H.A., Auster, R.E., Davies, K.H., Brown, C.M.L., 2021. Beaver: Nature's ecosystem engineers. WIREs Water 8, e1494. https://doi.org/10.1002/wat2.1494.
Breckheimer, I., 2019. 1 m Resolution Digital Elevation Model for the Upper Gunnison Domain Derived from 2015 and 2019 LiDAR Data.
Bush, S.A., Birch, A.L., Warix, S.R., Sullivan, P.L., Gooseff, M.N., McKnight, D.M., Barnard, H.R., 2023. Dominant source areas shift seasonally from longitudinal to lateral contributions in a montane headwater stream. J. Hydrol. 617, 129134 https://doi.org/10.1016/j.jhydrol.2023.129134.
Butler, D.R., 2012. Characteristics of beaver ponds on deltas in a mountain environment. Earth Surf. Process. Landf. 37, 876–882. https://doi.org/10.1002/esp.3218.
Butler, D.R., Malanson, G.P., 1995. Sedimentation rates and patterns in beaver ponds in a mountain environment. Geomorphol. Biogeomorphol. Terrest. Freshw. Syst. 13, 255–269. https://doi.org/10.1016/0169-555X(95)00031-Y.
Butler, D.R., Malanson, G.P., 2005. The geomorphic influences of beaver dams and failures of beaver dams. Geomorphology, Dams in Geomorphology 71, 48–60. https://doi.org/10.1016/j.geomorph.2004.08.016.
Cazzolla Gatti, R., Callaghan, T.V., Rozhkova-Timina, I., Dudko, A., Lim, A., Vorobyev, S. N., Kirpotin, S.N., Pokrovsky, O.S., 2018. The role of Eurasian beaver (Castor fiber) in the storage, emission and deposition of carbon in lakes and rivers of the river Ob flood plain, western Siberia. Sci. Total Environ. 644, 1371–1379. https://doi.org/10.1016/j.scitotenv.2018.07.042.
Cluer, B., Thorne, C., 2014. A stream evolution model integrating habitat and ecosystem benefits. River Res. Appl. 30, 135–154. https://doi.org/10.1002/rra.2631.
Davis, J., Lautz, L., Kelleher, C., Vidon, P., Russoniello, C., Pearce, C., 2021. Evaluating the geomorphic channel response to beaver dam analog installation using unoccupied aerial vehicles. Process. Landf. n/a, Earth Surf. https://doi.org/10.1002/esp.5180.
de Visscher, M., Nyssen, J., Pontzeele, J., Billi, P., Frankl, A., 2014. Spatio-temporal sedimentation patterns in beaver ponds along the Chevral river, Ardennes. Belgium. Hydrol. Process. 28, 1602–1615. https://doi.org/10.1002/hyp.9702.
Devito, K.J., Dillon, P.J., 1993. Importance of runoff and winter anoxia to the P and N dynamics of a beaver pond. Can. J. Fish. Aquat. Sci. 50, 2222–2234. https://doi.org/10.1139/f93-248.
Emlid, 2022. Reach RS2+ | Multi-band RTK GNSS Receiver for mapping [WWW Document], URL. https://emlid.com/reachrs2plus/ (accessed 4.28.23).
Frank, J.M., Fornwalt, P.F., Asherin, L.A., Alton, S.K., 2021. Manitou Experimental Forest Hourly Meteorology Data (3rd Edition). https://doi.org/10.2737/RDS-2011-0001-3.
Gaskill, D.L., DeLong Jr., J.E., Cochran, D.M., 1987. Geologic Map of the Mt. Axtell quadrangle, Gunnison County, Colorado (Geologic Map No. GQ-1604). United States Geological Survey. https://doi.org/10.3133/gq1604.
Giriat, D., Gorczyca, E., Sobucki, M., 2016. Beaver ponds' impact on fluvial processes (Beskid Niski Mts., SE Poland). Sci. Total Environ. 544, 339–353. https://doi.org/10.1016/j.scitotenv.2015.11.103.
Google Earth [WWW Document], 2022. URL. https://earth.google.com/web/@0,0,0a,22251752.77375655d,35y,0h,0t,0r (accessed 4.20.23).
Gurnell, A.M., 1998. The hydrogeomorphological e•ects of beaver dam-building activity. Prog. Phys. Geogr. Earth Environ. 22, 167–189. https://doi.org/10.1177/030913339802200202.
Harvey, J., Gooseff, M., 2015. River corridor science: hydrologic exchange and ecological consequences from bedforms to basins. Water Resour. Res. 51, 6893–6922. https://doi.org/10.1002/2015WR017617.
Hilton, S., Lisle, T.E., 1993. Measuring the fraction of pool volume filled with fine sediment (No. PSW-RN-414). U.S. Department of Agriculture, Forest Service, Pacific Southwest Research Station, Albany, CA. https://doi.org/10.2737/PSW-RN-414.
Hood, G.A., Larson, D.G., 2015. Ecological engineering and aquatic connectivity: a new perspective from beaver-modified wetlands. Freshw. Biol. 60, 198–208. https://doi.org/10.1111/fwb.12487.
Hua, Q., 2009. Radiocarbon: a chronological tool for the recent past. Quat. Geochronol. 4, 378–390. https://doi.org/10.1016/j.quageo.2009.03.006.
Hua, Q., Barbetti, M., 2004. Review of tropospheric bomb 14C data for carbon cycle modeling and age calibration purposes. Radiocarbon 46, 1273–1298. https://doi.org/10.1017/S0033822200033142.
Ives, R., 1942. The beaver-meadow complex. J. Geomorphol. 5, 191–203.
James, C.D., Lanman, R.B., 2012. Novel Physical Evidence that Beaver Historically Were Native to the Sierra Nevada. Calif, FISH GAME, p. 98.
John, S., Klein, A., 2004. Hydrogeomorphic effects of beaver dams on floodplain morphology: avulsion processes and sediment fluxes in upland valley floors (Spessart, Germany) [Les effets hydro-géomorphologiques des barrages de castors sur la morphologie de la plaine alluviale : processus d'avulsions et flux sédimentaires des vallées intra-montagnardes (Spessart, Allemagne).]. Quaternaire 15, 219–231. https://doi.org/10.3406/quate.2004.1769.
Johnston, C.A., 2014. Beaver pond effects on carbon storage in soils. Geoderma 213, 371–378. https://doi.org/10.1016/j.geoderma.2013.08.025.
Johnston, C.A., 2015. Fate of 150 year old beaver ponds in the Laurentian Great Lakes region. Wetlands 35, 1013–1019. https://doi.org/10.1007/s13157-015-0688-5.
Kramer, N., Wohl, E.E., Harry, D.L., 2012. Using ground penetrating radar to 'unearth' buried beaver dams. Geology 40, 43–46. https://doi.org/10.1130/G32682.1.
Landis, J.D., Renshaw, C.E., Kaste, J.M., 2016. Beryllium-7 and lead-210 chronometry of modern soil processes: the linked radionuclide aCcumulation model. LRC. Geochim. Cosmochim. Acta 180, 109–125. https://doi.org/10.1016/j.gca.2016.02.013.
Larsen, A., Larsen, J.R., Lane, S.N., 2021. Dam builders and their works: beaver influences on the structure and function of river corridor hydrology, geomorphology, biogeochemistry and ecosystems. Earth Sci. Rev. 218, 103623 https://doi.org/10.1016/j.earscirev.2021.103623.
Laurel, D., Wohl, E., 2019. The persistence of beaver-induced geomorphic heterogeneity and organic carbon stock in river corridors. Earth Surf. Process. Landf. 44, 342–353. https://doi.org/10.1002/esp.4486.
Levine, R., Meyer, G.A., 2014. Beaver dams and channel sediment dynamics on Odell Creek, Centennial Valley, Montana, USA. Geomorphology, Discontinuities in Fluvial Systems 205, 51–64. https://doi.org/10.1016/j.geomorph.2013.04.035.
Lininger, K.B., Wohl, E., Rose, J.R., 2018. Geomorphic controls on floodplain soil organic carbon in the Yukon flats, interior Alaska, from reach to River Basin scales. Water Resour. Res. 54, 1934–1951. https://doi.org/10.1002/2017WR022042.
McCreesh, R.K., Fox-Dobbs, K., Wimberger, P., Woodruff, K., Holtgrieve, G., Pool, T.K., 2019. Reintroduced beavers rapidly influence the storage and biogeochemistry of sediments in headwater streams (Methow River, Washington). Northwest Sci. 93, 112–121. https://doi.org/10.3955/046.093.0203.
Meentemeyer, R.K., Butler, D.R., 1999. Hydrogeomorphic effects of beaver dams in Glacier National Park. Montana. Phys. Geogr. 20, 436–446. https://doi.org/10.1080/02723646.1999.10642688.
Milliman, J.D., Syvitski, J.P.M., 1992. Geomorphic/tectonic control of sediment discharge to the ocean: the importance of small mountainous Rivers. J. Geol. 100, 525–544. https://doi.org/10.1086/629606.
Murray, D., Neilson, B.T., Brahney, J., 2021. Source or sink? Quantifying beaver pond influence on non-point source pollutant transport in the intermountain west. J. Environ. Manag. 285, 112127 https://doi.org/10.1016/j.jenvman.2021.112127.
Naiman, R.J., Melillo, J.M., Hobbie, J.E., 1986. Ecosystem alteration of boreal Forest streams by beaver (Castor Canadensis). Ecology 67, 1254–1269. https://doi.org/10.2307/1938681.
Norman, L.M., Lal, R., Wohl, E., Fairfax, E., Gellis, A.C., Pollock, M.M., 2022. Natural infrastructure in dryland streams (NIDS) can establish regenerative wetland sinks that reverse desertification and strengthen climate resilience. Sci. Total Environ. 849, 157738 https://doi.org/10.1016/j.scitotenv.2022.157738.
Nummi, P., Vehkaoja, M., Pumpanen, J., Ojala, A., 2018. Beavers affect carbon biogeochemistry: both short-term and long-term processes are involved. Mammal Rev. 48, 298–311. https://doi.org/10.1111/mam.12134.
Oberle, W., 2015. Monte Carlo Simulations: Number of Iterations and Accuracy.
Ortega, J., Turnipseed, A., Guenther, A.B., Karl, T.G., Day, D.A., Gochis, D., Huffman, J. A., Prenni, A.J., Levin, E.J.T., Kreidenweis, S.M., DeMott, P.J., Tobo, Y., Patton, E.G., Hodzic, A., Cui, Y.Y., Harley, P.C., Hornbrook, R.S., Apel, E.C., Monson, R.K., Eller, A.S.D., Greenberg, J.P., Barth, M.C., Campuzano-Jost, P., Palm, B.B., Jimenez, J.L., Aiken, A.C., Dubey, M.K., Geron, C., Offenberg, J., Ryan, M.G., Fornwalt, P.J., Pryor, S.C., Keutsch, F.N., DiGangi, J.P., Chan, A.W.H., Goldstein, A. H., Wolfe, G.M., Kim, S., Kaser, L., Schnitzhofer, R., Hansel, A., Cantrell, C.A., Mauldin, R.L., Smith, J.N., 2014. Overview of the Manitou experimental Forest Observatory: site description and selected science results from 2008 to 2013. Atmos. Chem. Phys. 14, 6345–6367. https://doi.org/10.5194/acp-14-6345-2014.
Parker, G., 1937. The Parker Document.
Pearce, C., Vidon, P., Lautz, L., Kelleher, C., Davis, J., 2021. Short-term impact of beaver dam analogues on streambank erosion and deposition in semi-arid landscapes of the Western USA. River Res. Appl. 37, 1032–1037. https://doi.org/10.1002/rra.3825.
Persico, L., Meyer, G., 2009. Holocene beaver damming, fluvial geomorphology, and climate in Yellowstone national park. Wyoming. Quat. Res. 71, 340–353. https://doi.org/10.1016/j.yqres.2008.09.007.
Phillips, J.M., Russell, M.A., Walling, D.E., 2000. Time-integrated sampling of fluvial suspended sediment: a simple methodology for small catchments. Hydrol. Process. 14, 2589–2602. https://doi.org/10.1002/1099-1085(20001015)14:14<2589::AID-HYP94>3.0.CO;2-D.
Pollock, M.M., Heim, M., Werner, D., 2003. Hydrologic and Geomorphic Effects of Beaver Dams and Their Influence on Fishes 23.
Pollock, M.M., Beechie, T.J., Jordan, C.E., 2007. Geomorphic changes upstream of beaver dams in Bridge Creek, an incised stream channel in the interior Columbia River basin, eastern Oregon. Earth Surf. Process. Landf. 32, 1174–1185. https://doi.org/10.1002/esp.1553.
Pollock, M.M., Beechie, T.J., Wheaton, J.M., Jordan, C.E., Bouwes, N., Weber, N., Volk, C., 2014. Using beaver dams to restore incised stream ecosystems. BioScience 64, 279–290. https://doi.org/10.1093/biosci/biu036.
Polvi, L.E., Wohl, E., 2012. The beaver meadow complex revisited – the role of beavers in post-glacial floodplain development. Earth Surf. Process. Landf. 37, 332–346. https://doi.org/10.1002/esp.2261.
Puttock, A., Graham, H.A., Carless, D., Brazier, R.E., 2018. Sediment and nutrient storage in a beaver engineered wetland. Earth Surf. Process. Landf. 43, 2358–2370. https://doi.org/10.1002/esp.4398.
Ryan, J.N., Bevan, H., Dodge, C., Norvell, A., 2009. Sources of Metal Contamination in the Coal Creek Watershed, Crested Butte, Gunnison County, Colorado: Part III. Early Spring Flow, April 2007.
Scamardo, J., Wohl, E., 2020. Sediment storage and shallow groundwater response to beaver dam analogues in the Colorado front range, USA. River Res. Appl. 36, 398–409. https://doi.org/10.1002/rra.3592.

Scott, D.N., Wohl, E.E., 2018. Geomorphic regulation of floodplain soil organic carbon concentration in watersheds of the rocky and Cascade Mountains, USA. Earth Surf. Dyn. 6, 1101–1114. https://doi.org/10.5194/esurf-6-1101-2018.

Stuiver, M., Reimer, P.J., 1993. Extended 14C Data Base and revised CALIB 3.0 14C age calibration program. Radiocarbon 35, 215–230. https://doi.org/10.1017/S0033822200013904.

Sutfin, N.A., Wohl, E.E., Dwire, K.A., 2016. Banking carbon: a review of organic carbon storage and physical factors influencing retention in floodplains and riparian ecosystems. Earth Surf. Process. Landf. 41 38-60 41, 38–60. https://doi.org/10.1002/esp.3857.

Sutfin, N.A., Wohl, E., Fegel, T., Day, N., Lynch, L., 2021. Logjams and channel morphology influence sediment storage, transformation of organic matter, and carbon storage within mountain stream corridors. Water Resour. Res. 57, e2020WR028046 https://doi.org/10.1029/2020WR028046.

Tweto, O., 1979. Geologic Map of Colorado.

USACE National Inventory of Dams [WWW Document], 2022. URL. https://nid.usace.army.mil/#/ accessed 4.15.22.

USGS Current Water Data for the Nation [WWW Document], 2022. URL. https://waterdata.usgs.gov/nwis/rt accessed 4.12.23.

USGS EarthExplorer [WWW Document], 2021. URL. https://earthexplorer.usgs.gov/ accessed 4.17.22.

USGS SNOTEL, Butte (380) - [WWW Document], 2023. URL. https://wcc.sc.egov.usda.gov/nwcc/site?sitenum=380 (accessed 3.28.23).

Westbrook, C.J., Cooper, D.J., Baker, B.W., 2011. Beaver assisted river valley formation. River Res. Appl. 27, 247–256. https://doi.org/10.1002/rra.1359.

Weyhenmeyer, C.E., 1999. Methane emissions from beaver ponds: rates, patterns, and transport mechanisms. Global Biogeochem. Cycles 13, 1079–1090. https://doi.org/10.1029/1999GB900047.

Wohl, E., 2013. Landscape-scale carbon storage associated with beaver dams. Geophys. Res. Lett. 40, 3631–3636. https://doi.org/10.1002/grl.50710.

Yarnell, S., Pope, K., Wolf, E., Burnett, R., Wilson, K., 2020. A Demonstration of the Carbon Sequestration and Biodiversity Benefits of Beaver and Beaver Dam Analogue Restoration Techniques in Childs Meadow, Tehama County, California (Technical Report No. CWS-2020-01). Center for Watershed Sciences, UC Davis.